

## Performance of double reinforced concrete panel against blast hazard

Mostafa M. A. Wahab<sup>a</sup> and Sherif A. Mazek\*

*Civil Engineering Department, Military Technical College, Cairo, Egypt*

*(Received December 30, 2015, Revised July 13, 2016, Accepted July 29, 2016)*

**Abstract.** Terrorist attacks have used conventional high explosives. Such attacks need the development of blast resistant construction. Most of sandwich panels used in protection purpose have the capability of dissipating energy by large plastic deformation under blast loading. These sandwich panels could not resist repetitive explosions. This panel should be replaced with new one to resist another explosion event. The aim of this study is to use double reinforced concrete panels to achieve high resistance against different explosion charges and to resist repetitive explosion shots. This sandwich panel is composed of two reinforced concrete slabs connected by number of helical springs. The blast field test is carried out. The finite element analysis (FEA) is also used to model the double reinforced concrete panels under shock wave. The performance of the double reinforced concrete panel is studied based on detonating different TNT explosive charges. There is a good agreement between the results obtained by both the field blast test and the numerical simulation. The spring improves the double reinforced concrete panel performance under the blast wave propagation.

**Keywords:** displacements; finite element analysis; field blast test; double reinforced concrete panels; springs; TNT explosive charge

---

### 1. Introduction

Understanding of blast impact provides blast protection for civilian structures (Aimone 1982; Liu and Katsabanis 1997; Fayad 2009; Mohamad 2006; Schueller 1991; Zhang and Valliappan 1990). There is a need to understand both dynamic interaction of blast loading with structures and shock mitigating mechanisms. Traditional lightweight materials are used as effective materials for blast protection applications because of their ability to mitigate shock wave applied to structures due to terrorist attacks (Liu and Katsabanis 1997; Gustafsson 1973; Technical Manual TM 5-885-1 1986; Technical Manual TM 5-1300 2008). To better understand structural damage under blast load conditions, many researches conducted studies on the protection of civilian structures against blast wave (Fayad 2009; Mohamad 2006; Beshara 1994; Liane and Hedman 1999; Smith and Hetherington 1994; Wu *et al.* 1999). The composite structures become an engineering challenge to understand their performance against blast effect.

---

\*Corresponding author, Professor, E-mail: samazek@yahoo.com

<sup>a</sup>E-mail: mmmawahab@yahoo.com

It is very expensive to conduct field blast tests in every site and sometimes it is impossible to carry out such field tests due to safety and environmental constraints (Dharmasena *et al.* 2008; Hao *et al.* 1998). However, a reliable numerical model validated with measured field data is an effective tool to analyze the structure performance under blast effect (Dharmasena *et al.* 2008; Hao *et al.* 1998; Ming 2008; Rashad 2014).

Chen and Chen (1996) investigated the dynamic soil-structure interaction phenomenon involved in shallow-buried flexible plate under impact load. They used the experimental and the numerical works to study the performance of the buried structure. Lu *et al.* (2005) used a fully coupled numerical model to simulate the response of buried concrete structure under subsurface blast. The responses of the buried structure obtained by 2-D numerical model at different points were compared by those obtained by 3-D numerical model. Trelat *et al.* (2007) studied impact of shock wave on structure due to explosion at altitude. They improved the understanding of interaction of blast waves with both ground and structure using both the FEA and the experimental work. Luccioni *et al.* (2009) studied craters produced by underground explosions. They discussed the accuracy of numerical simulation of craters produced by underground explosions. Yaghin *et al.* (2009) investigated the responses of damaged reinforced concrete members to dynamic excitation and to identify the location of probable defects. They used finite element analysis to analyze the damaged cantilever beams.

Ha *et al.* (2011) used carbon fiber reinforced polymer (CFRP) to strengthen structures against blast load. They conducted an experimental work on CFRP to strengthen RC panels under blast loading. Asha and Sundarajan (2014) used a nonlinear finite element analysis to evaluate seismic behavior of reinforced concrete exterior-beam-column joints. They compared the numerical results with the experimental results under cyclic loading. Bencardino and Condello (2014) evaluated behavior and strength of steel reinforced grout externally strengthened reinforced concrete beams by using a 3-D nonlinear numerical analysis. The reliability of the 3-D finite element model was checked using experimental data obtained on set of three RC beams. Marzec *et al.* (2015) presented results of finite element simulations of the strain-rate concrete behavior under dynamic loading. A decrease of the material stiffness was considered for a very high velocity generated form dynamic loading.

In this study, the performance of the double reinforced concrete (DRC) panel connected by the helical springs is evaluated under the impact of the blast wave load. The DRC panel could be also used to resist the structure from repetitive explosion events. The 3-D numerical model is proposed using finite element analysis (FEA) to study the spring performance for strengthening the effect on the DRC panel, as shown in Fig. 1. The DRC panel connected by springs are used to study blast mitigation for the reinforced concrete slabs with constant thickness. The DRC panel consists of two reinforced concrete slabs connected by the helical springs, as shown in Fig. 1. The upper RC slab facing the blast explosion is considered as protection layer. The lower RC slab is considered as the slab needing protection from blast effect, as shown in Fig. 1. The thickness of each reinforced concrete slab is 10 cm. The single reinforced concrete slab is also tested under blast effect to study the impact of the helical springs on the lower RC slab performance of the DRC slab. The single reinforced concrete slab is considered in this study as control slab (control panel). In this study, nine helical springs are used to connect the two RC panels, as shown in Fig. 1. The diameter of helical wire spring is 2 cm. The outer diameter of the helical spring is 15 cm. The patch distance of the helical wire spring is 4.6 cm. The spring stiffness (K) is chosen to be 15 t/m. However, the helical springs are used to absorb the blast wave energy so as to protect the lower RC panel from the blast effect.

Field blast test is also conducted to record pressure-time history of blast wave hitting the sandwich steel panel and to record maximum displacement at the centre point of the lower RC slab, as shown in Fig. 1. The study presents a comparison between the results obtained from both the blast field test and the numerical model to validate the accuracy of the 3-D finite element analysis (FEA). The constitutive model for this analysis is elasto-plastic model. An elasto-plastic model is employed to represent the performance of the DRC panel. The proposed model is programmed and linked to commercial blast computer program Autodyn-3D (2005). The DRC panels' model connected by the springs is also implemented in a finite element code Autodyn-3D, as shown in Fig. 2. Current codes and regulations to estimate blast wave intensities due to outdoor blasting are also used in this study based on empirical methods (Gustafsson 1973; Technical Manual TM 5-1300 2008; Remennikov 2003). These empirical methods were obtained from observations and measurements in blast field tests.

The finite element model takes into account the effect of the blast load, the DRC panels, and the springs. The effect is expressed in terms of the displacement-time history of the lower RC slab as the explosive wave propagates. The 3-D nonlinear FEA is conducted to study the impact of the springs on the performance of the DRC panels based on different TNT charges. The behavior of the DRC panels is investigated under the blast waves obtained from detonating 1-kg, 5-kg, and 10-kg TNT explosive charges at a stand-off distance ( $R$ ) of 1 m. However, the pressure time histories generated by the TNT charge weight and the stand-off distance are selected to be compatible with the stiffness of the helical springs between the DRC panel so as to protect the lower RC slab from blast effect.

Numerical results obtained by the FEA are compared with the data obtained from the field blast test. The numerical model could be used to predict the blasting-induced pressure on the DRC panels. The maximum displacements of the DRC panels are recorded and computed by the authors.

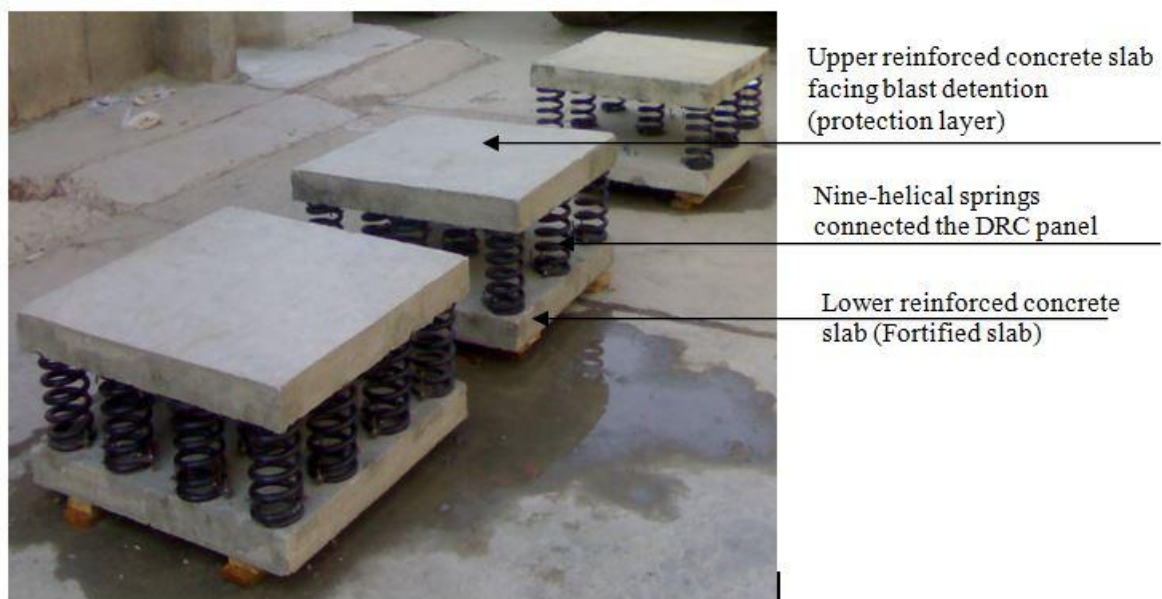


Fig. 1 Fabricated double reinforced concrete panels connected by springs

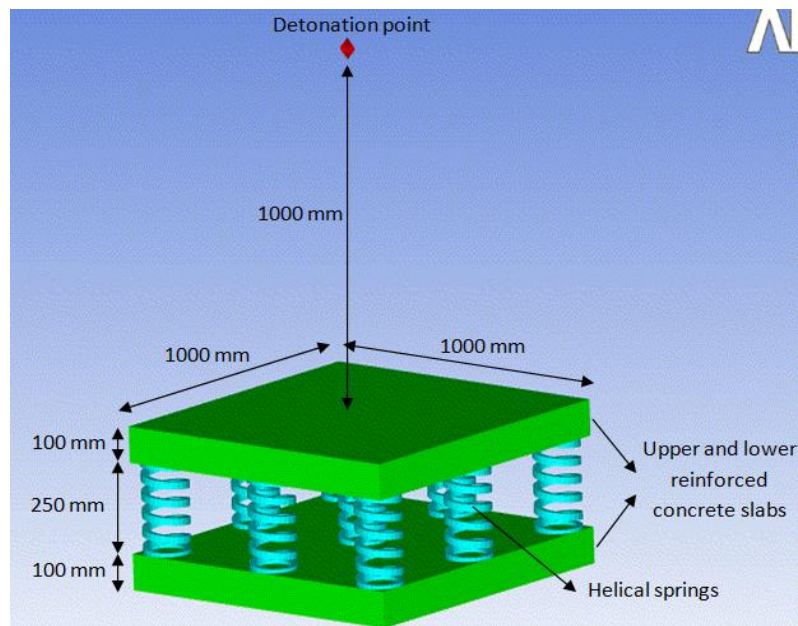


Fig. 2 3-D model of double reinforced concrete panels connected by springs

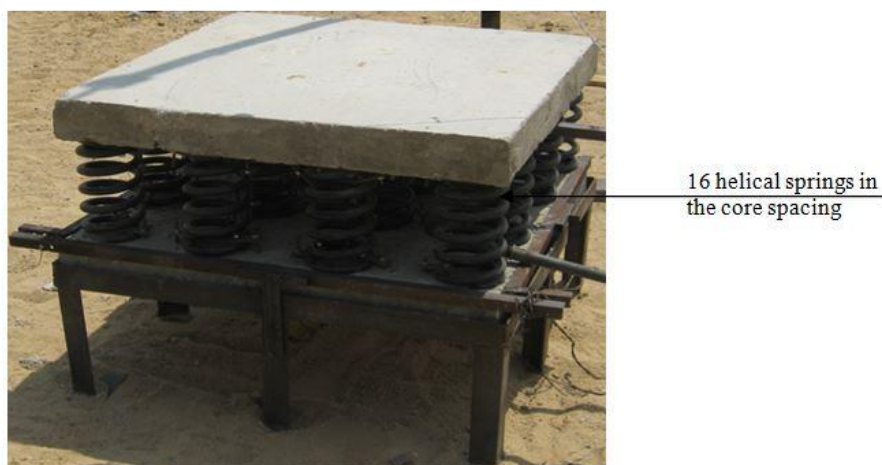


Fig. 3 Test rig supports the double reinforced concrete panels

## 2. Blast field test

A field test rig is manufactured to support specimens. The test rig carries the specimen from the lower reinforced concrete slab of the DRC panels, as shown in Fig. 3. The dimension of the test rig is 1.03 m×1.03 m and the height of the test rig is 0.3 m above ground surface. The DRC panel is subjected to different TNT charges at stand-off distance of 1 m measured from the upper reinforced concrete slab of the DRC panel. The boundary conditions of the field test are considered to satisfy free air explosion effect on the specimens.



Fig. 4 Measurement instrumentation for field blast test



Fig. 5 Pressure sensor and cable protective system

The measurement instrument used at the field blast test is shown in Fig. 4. The sensor interface (transducer) PCD-320A is a voltage measuring instrument which is connected to the personal computer via the USB port in order to record pressure-time history due to blast load. This device is capable of measuring voltage attached to control software. Each sensor interface provides 4 channels, as shown in Fig. 4. Piezotronics PCB pressure smart sensor is a sensor used to receive the incident pressure resulting from blast wave propagation, as shown in Fig. 4. The detected signals are amplified and transmitted to data acquisition system to record the pressure-time history. Fig. 4 shows the amplifier used to enlarge the volt signals received from pressure sensor to the

transducer. Steel tube is used to protect the pressure sensor cables from damaging, as shown in Fig. 5. The maximum displacements of the lower RC slab are also measured under blast loading. LVDTs are placed at the centre of the lower RC slab to record maximum displacement at the centre of the lower RC slab.

### 3. Double Reinforced Concrete (DRC) panel model

The studied DRC panel is composed of outer two reinforced concrete slabs. The dimensions of each concrete slab are 1 m in width, 1 m in length, and 0.1 m in thickness. The core spacing between the two reinforced concrete slabs is filled with different numbers of helical springs. The core spacing is 250 mm, as shown in Fig. 2. To study the blast response of the DRC panel subjected to blast loading, finite element model is developed using Autodyn-3D, which coincides with the finite element program ANSYS. The DRC panel with nine helical springs in the core spacing is considered in this study, as shown in Fig. 3. The helical springs used at the DRC panel is used to absorb the blast wave propagation.

The DRC panel consists of the two reinforced concrete slabs reinforced by steel reinforcement mesh of 5  $\emptyset$  8 /m. The core spacing has nine compression helical steel springs. The mechanical properties of reinforced steel bars and springs used in FEA are Poisson's ratio  $\nu$  of 0.3, average mass steel density of 7900 kg/m<sup>3</sup>, elastic modulus (E) of 2350 t/cm<sup>2</sup>, and yield strength ( $f_y$ ) of 3600 kg/cm<sup>2</sup>. The steel spring stiffness is considered to be 15 t/m<sup>3</sup>. The diameter of helical wire spring is 20 mm. The outer diameter of the helical spring is 15 cm. The nine helical springs and the DRC panels are connected to each other. The shear modulus of the steel depends on the elastic modulus (E) and Poisson's ratio  $\nu$ .

The mechanical properties of concrete used in the finite element analysis are Poisson's ratio ( $\nu$ ) of 0.17; concrete density of 2250 kg/m<sup>3</sup>; compressive strength ( $f_c$ ) of 350 kg/cm<sup>2</sup>, elastic modulus (E) of 220 t/cm<sup>2</sup>. The shear modulus of the steel depends on the elastic modulus E and Poisson's ratio  $\nu$ .

The lower reinforced concrete slab is simply supported and restrained from translation in all directions at the perimeter nodes. Two reinforced concrete slabs and springs in the interior space are bounded to each others. The DRC panel and the TNT explosion are surrounded by air. The boundary condition of the air is called flow out media which permits to translate blast wave in air media as in the blast field test. Fig. 6 illustrates the boundary conditions of the lower reinforced concrete slab and the air media at which the blast wave propagates.

In the numerical modeling, the air and the TNT are simulated by Euler processes. The DRC panel is simulated by Lagrange processes (Dharmasena *et al.* 2008; Hao *et al.* 1998; Ming 2008). Steel reinforcement bars of the DRC panel are modeled by 3-D beam elements. The 3-D Beam elements are also used to model spring element in the 3-D finite element analysis, as shown in Fig. 7.

Cubic solid element is used to model the behavior of the lower RC slab and the upper RC slab, as shown in Fig. 6. In this study, the DRC panel strengthened by the helical springs is modeled. 20-node solid elements are used for modeling the lower and the upper slabs of the DRC panel with each node having 3 degrees of freedom (three translations).

The solid element and the 3-D beam element are used between the DRC panel and the springs to ensure the compatibility conditions at the interface between them as well as the associated stresses and strains along the interface surface.

#### 4. Blast wave impact

In numerical modeling, air and equivalent explosive TNT are simulated by Euler processor, as shown in Fig. 6. The air and the equivalent explosive TNT are assumed to satisfy the equation of state (EOS) of ideal gas (Hao *et al.* 1998). The DRC is modeled by the modified isotropic damage model and simulated by Lagrange processor (Hao *et al.* 1998, Wu *et al.* 1999), as shown in Fig. 6. The whole domain including the air media, the DRC, the helical springs, and the TNT explosive is shown in Fig. 6. Transmitting boundary is used to reduce reflection of stress wave from the numerical boundaries. The standard constants of air and TNT charge are obtained from the Autodyn-3D material library. These include air mass density  $\rho = 1.225 \text{ kg/m}^3$ ; air initial internal energy  $E_n = 2.068 \times 10^5 \text{ kJ/kg}$ ; and ideal air constant  $\gamma = 1.4$ . It should also be noted that viscous damping effect is neglected in the numerical simulation as its influence on high velocity explosion-type responses is insignificant (Hao *et al.* 1998; Wu *et al.* 1999).

The shock of the blast wave is generated when the surrounding atmosphere is subjected to an extreme compressive pulse radiating outward from the centre of the explosion. Transient pressure being greater than ambient pressure is defined as the overpressure ( $P_s$ ) (Smith and Hetherington 1994). The peak overpressure ( $P_s$ ) is the maximum value of the overpressure at a given location. The rise time to peak overpressure is less than microsecond (Baker *et al.* 1983).

In the current study, the field blast test is conducted to measure the pressure-time history at points (2) and (3) and to only measure the maximum displacement at point (4), as shown in Fig. 8. The further study is extended to only compute the pressure-time history at point (4). The measured pressure-time history at points (2) and (3) and the measured maximum displacements at point (4) are used to verify the 3-D numerical model. The blast detonation is very dangerous process and requires high special cautions according to Egyptian commandment so as to protect the environmental condition. The study presents a comparison between the pressure-time histories obtained by the field blast test and by the Autodyn-3D hydro code (numerical model) at points (2) and (3), as shown in Fig. 8.

One-kg TNT, five-kg TNT, and ten-kg TNT explosive charges are applied at stand-off distance of one meter to obtain the pressure-time history hitting the DRC panel by the numerical model and the field blast test at points (2) and (3), as shown in Fig. 8. Point (2) is located at the center of the upper surface of the upper concrete slab facing the blast effect. Point (3) is located at the mid height of the core spacing center. Point (4) is located at the center of the back surface of the lower concrete slab. Point (6) is located at the center of the back surface of the upper concrete slab. The computed and the recorded pressure-time histories at point (3) using one-kg TNT explosive charge are shown in Fig. 9. The computed and the recorded pressure-time histories at point (2) using five-kg TNT and ten-kg TNT explosive charges are also shown in Figs. 10 and 11. The result reveals that the results obtained by the field blast test agree 90% with respect to those estimated by the numerical model. The pressure-time histories at point (4) are also computed and presented in Figs. 12 and 13 based on five-kg TNT and ten-kg TNT explosive charges.

#### 5. Impact of springs on performance of DRC panel

The displacement-time history of the DRC panel including the helical springs due to blast load is calculated using the 3-D FEA. The blast wave propagation hits the DRC panel. The blast loads affecting the DRC panel are shown in Figs. 9 to 13. The study discusses the impact of the

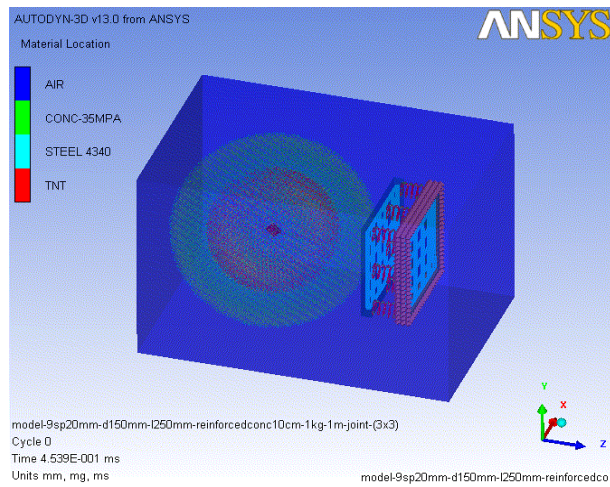


Fig. 6 3-D numerical model of DRC panel, springs, and TNT charge, and air media

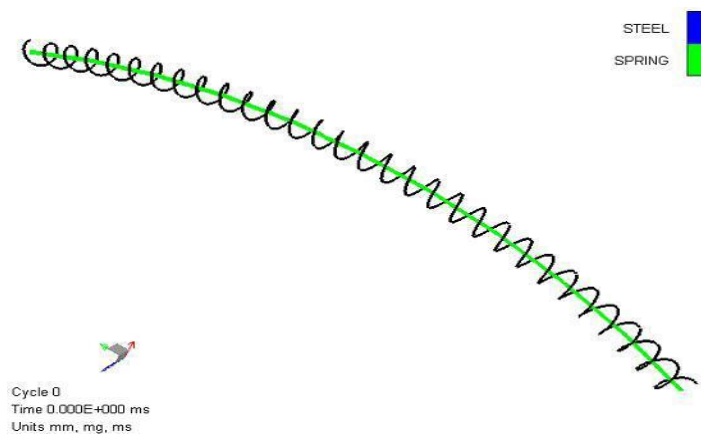


Fig. 7 3-D Beam element for spring

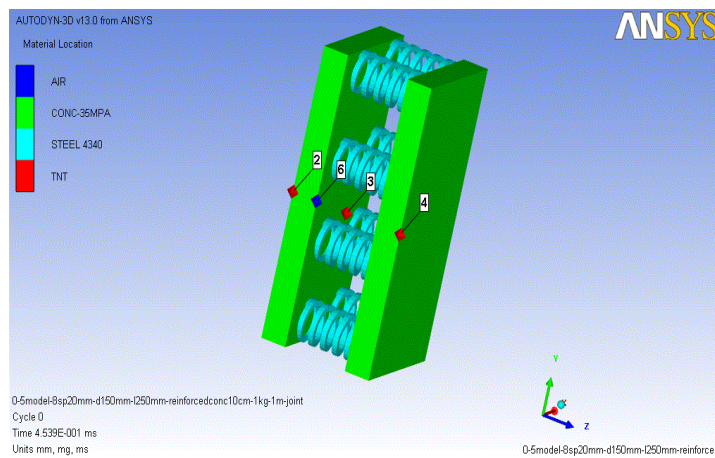


Fig. 8 Points 2, 3, 4, and 6 located in a half model of the DRC panel including helical spring at the core space

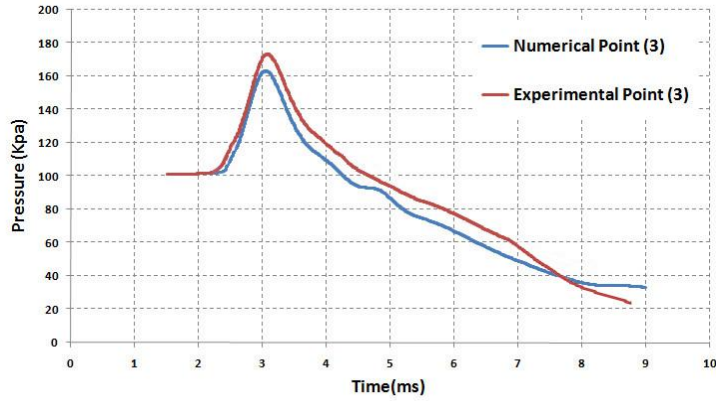


Fig. 9 Recorded and computed pressure-time histories hitting the DRC panel at point 3 based on 1-kg TNT explosive at stand-off distance (R) of 1 m

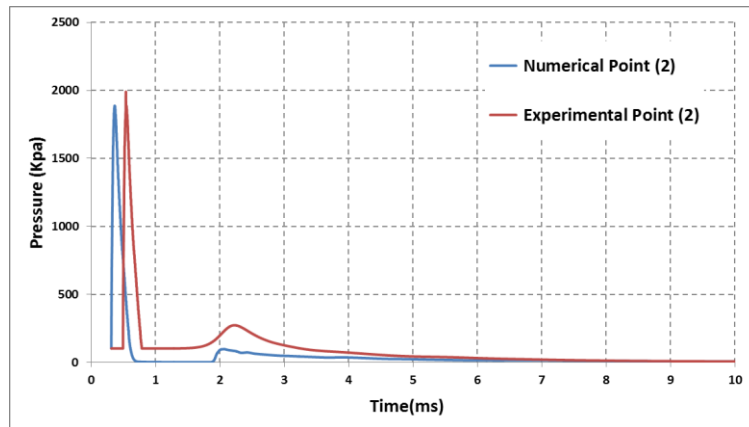


Fig. 10 Recorded and computed pressure-time histories hitting the DRC panel at point 2 based on 5-kg TNT explosive at stand-off distance (R) of 1 m

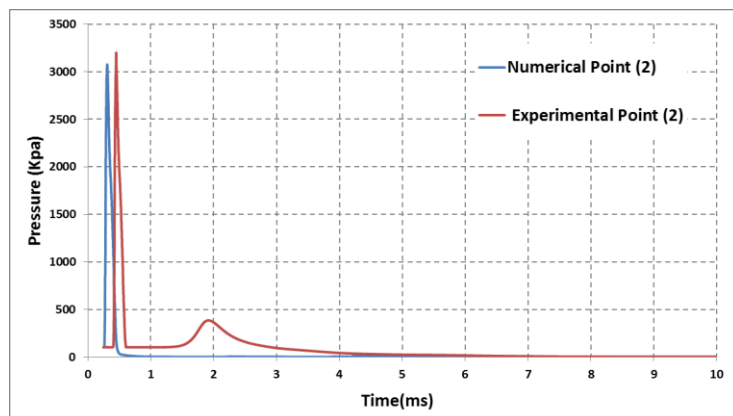


Fig. 11 Recorded and computed pressure-time histories hitting the DRC panel at point 2 based on 10-kg TNT explosive at stand-off distance (R) of 1 m

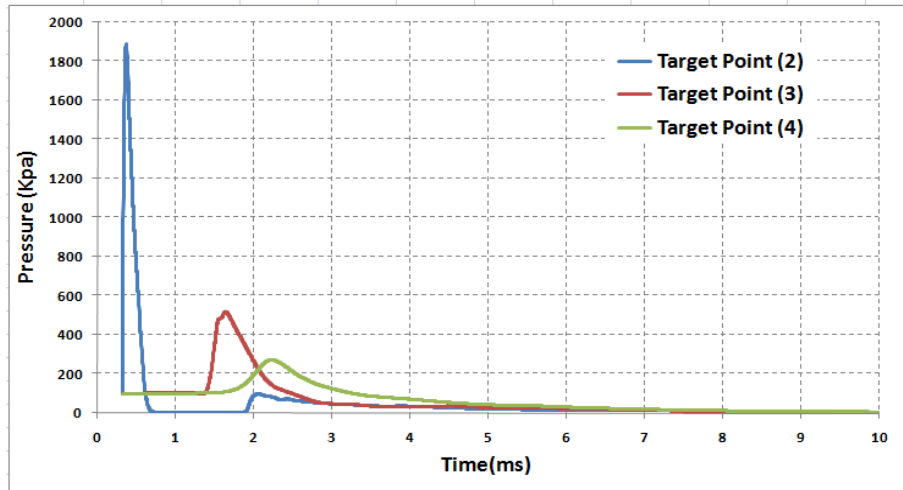


Fig. 12 Computed pressure-time histories hitting the DRC panel at points 2, 3, and 4 based on 5-kg TNT explosive at stand-off distance (R) of 1 m

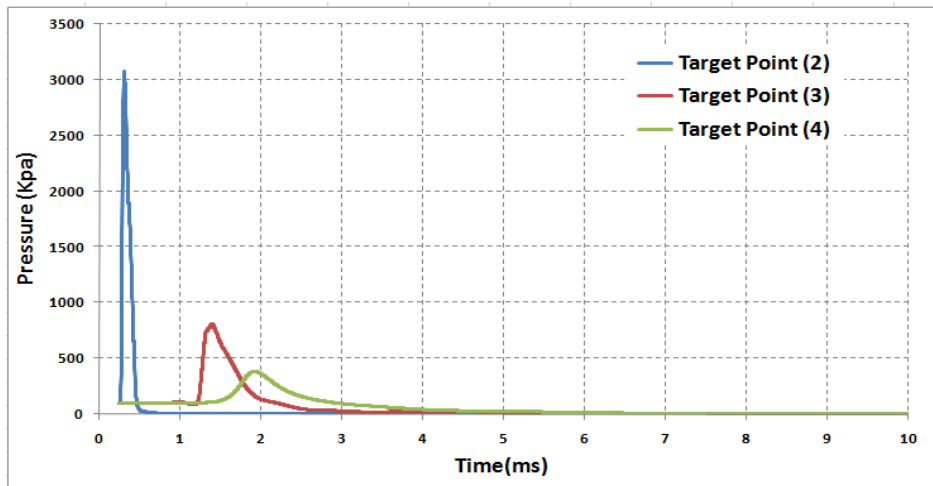


Fig. 13 Computed pressure-time histories hitting the DRC panel at points 2, 3, and 4 based on 10-kg TNT explosive at stand-off distance (R) of 1 m

springs at the core space on the DRC panel performance under the blast impact. Four specimens are tested in the field to record the maximum displacement at point (4) based on different TNT charges.

For the first test, four-kg TNT explosive is used to study the performance of the control reinforced concrete panel (Fig. 8). The control reinforced concrete panel is single reinforced concrete slab without helical springs. The four-kg TNT explosive is located at the one-meter stand-off distance from the control reinforced concrete panel (specimen No. 1), as shown in Fig. 14. The field blast test shows that the control reinforced concrete slab is totally damaged, as shown in Fig. 15. However, the control RC panel could not resist the blast effect and can not be used under repetitive loads. Thus, the following specimens will use helical springs to absorb the blast wave energy so as to protect the fortified RC panel from damage.



Fig. 14 Specimen No. 1 is subjected to four-kg TNT at stand-off distance of 1m (Control RC panel without helical springs)



Fig. 15 Specimen No. 1 after subjecting to four-kg TNT explosive charge (Control RC panel without helical springs)

For the second test, one-kg TNT explosive is used to discuss the impact of the nine springs on the DRC panel at points (4) and (6) (upper and lower reinforced concrete slabs) (Fig. 8). The TNT explosive is located at the one-meter stand-off distance from the DRC panel (specimen No. 2), as

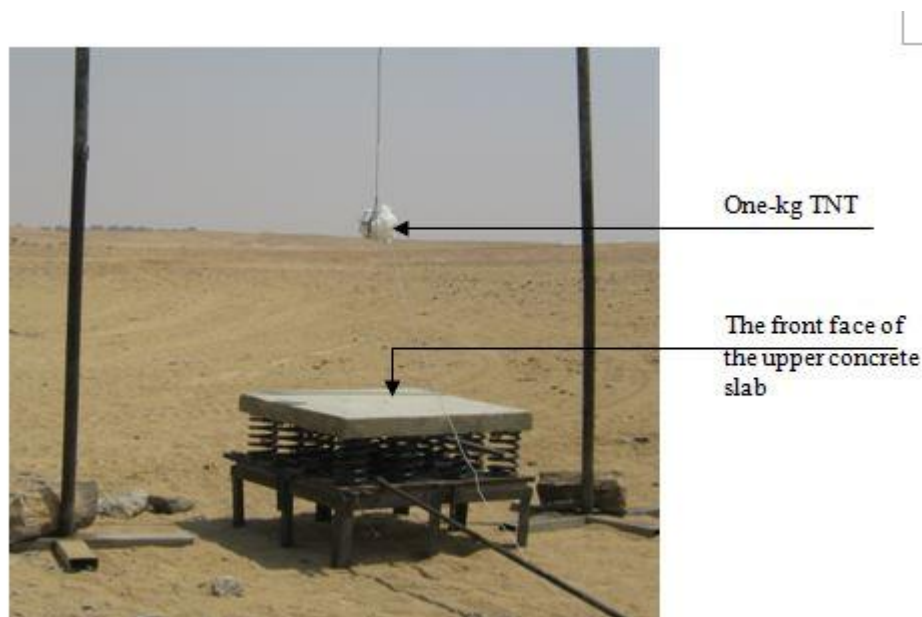


Fig. 16 Specimen No. 2 is subjected to one-Kg TNT at stand-off distance of 1m

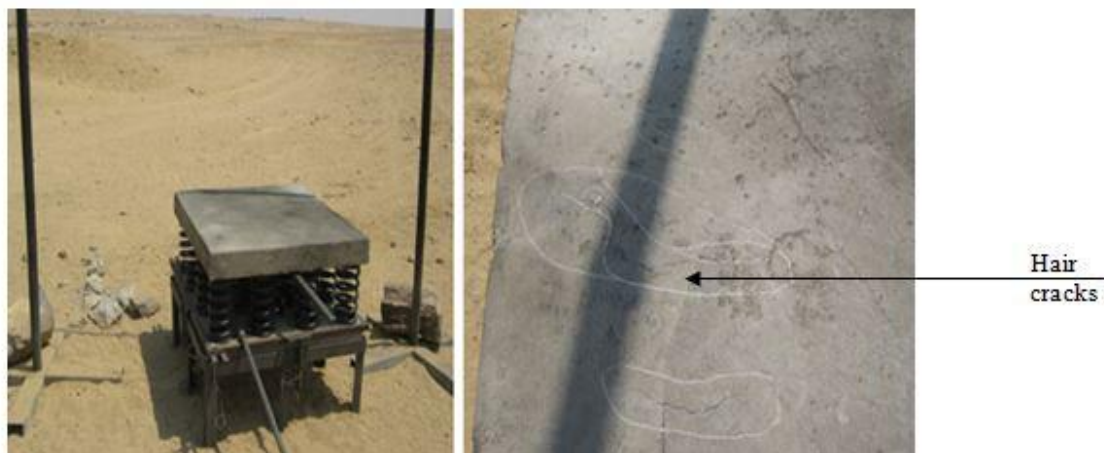


Fig. 17 Specimen No. 2 after subjecting to one-kg TNT explosive charge

shown in Fig. 16. The pressure- time history hitting the DRC panel is presented in Fig. 9. The field blast test shows that there are hair cracks appear on the front surface of the upper reinforced concrete slab and there is no hair crack occurred on the lower reinforced concrete slab, as shown in Fig. 17. The maximum displacement at point (4) located at the center of the back surface of the lower concrete slab is also recorded and presented in Table 1. The maximum computed displacement at point (4) is compared with the maximum recorded displacement at point (4) as tabulated in Table 1.

For the third test, five-kg TNT explosive at stand-off distance of 1 m is used to discuss the impact of the springs on the DRC panel at points (4) and (6) (Fig. 8). The TNT explosive is

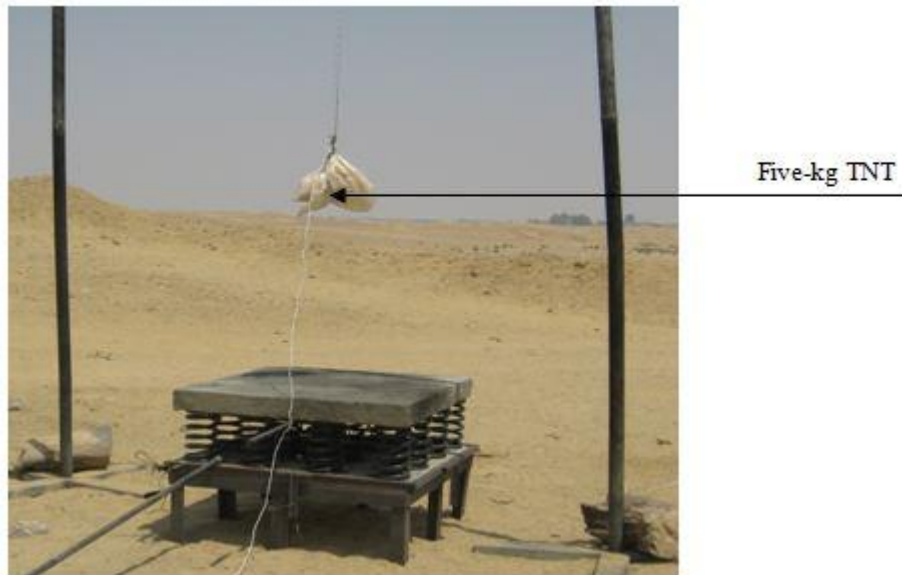


Fig. 18 Specimen No. 3 is subjected to five-Kg TNT at stand-off distance of 1m



Fig. 19 Specimen No. 3 after subjecting to five-kg TNT explosive charge (Significant cracks appears through protection layer)

located at the one-meter stand-off distance from the DRC panel (specimen No. 3), as shown in Fig. 18. The pressure- time history hitting the DRC panel is presented in Fig. 12. The field blast test shows that there are significant cracks appear through the upper reinforced concrete slab and on its sides and there is no cracks occurred on the lower reinforced concrete slab, as shown in Fig. 19. The maximum displacement at point (4) is also recorded and presented in Table 1 using five-kg TNT explosive. The maximum computed displacement at point (4) is also compared with the maximum recorded displacement at point (4) as tabulated in Table 1.



Fig. 20 Specimen No. 4 is subjected to ten-Kg TNT at stand-off distance of 1m



Fig. 21 Specimen No. 4 after subjecting to ten-kg TNT explosive charge

For the fourth test, ten-kg TNT explosive is used to discuss the impact of the springs on the DRC panel at points (4) and (6) (Fig. 8). The TNT explosive is located at the one-meter stand-off distance from the DRC panel (specimen No. 4), as shown in Fig. 20. The pressure-time history hitting the DRC panel is presented in Fig. 13. The field blast test shows that the upper reinforced concrete slab is totally damaged and fragmented into pieces and there is no cracks occurs on the lower reinforced concrete slab, as shown in Fig. 21. The maximum displacement at point (4) is also recorded and presented in Table 1 based on using ten-kg TNT explosive. The maximum computed displacement at point (4) is also compared with the maximum recorded displacement at point (4) as tabulated in Table 1.

Table 1 Maximum displacement at the centre of the fortified (lower) reinforced concrete slab (point 4) under different TNT explosives at stand-off distance (R) of 1 m

Sample	TNT explosive (kg)	Maximum recorded displacement obtained by the field blast test (mm)	Maximum computed displacement obtained by the FEA (mm)
Control panel	4 (Specimen No. 1)	Complete damaged (55 mm)	Complete damaged
	1 (Specimen No. 2)	3	2.8
DRC panel	5 (Specimen No. 3)	6.2	5.8
	10 (Specimen No. 4)	10.6	9.9

Note: DRC is double reinforced concrete panel

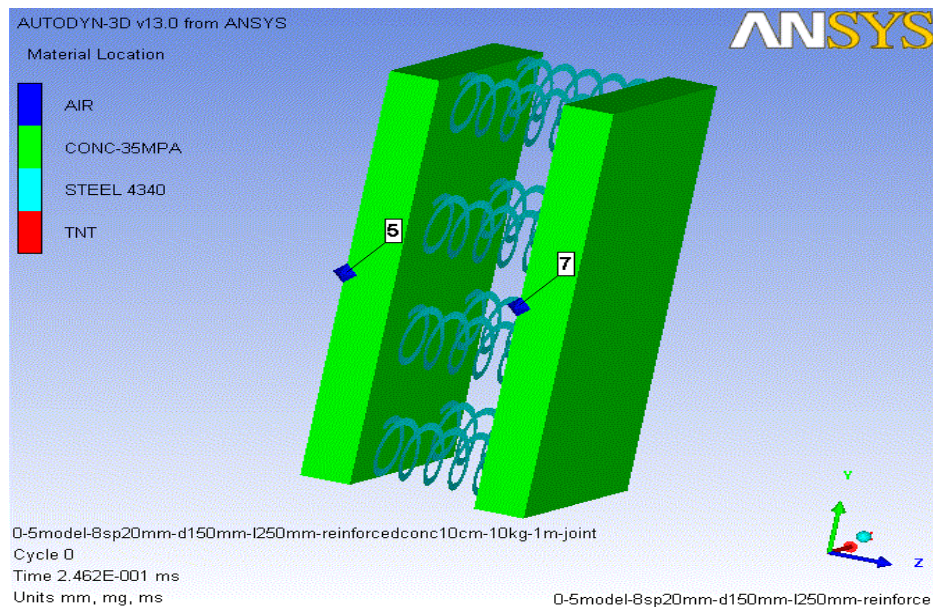


Fig. 22 Points 5 and 7 located in a half model of the DRC panel including helical spring at the core space

Using four-kg TNT explosive charge, the maximum displacement of the control RC slab at point (4) is computed to discuss the impact of the helical springs, as presented in Table 1. The maximum displacement of the control RC slab at point (4) is also obtained by the field blast test as presented in Table 1. The result indicates that the control RC slab is completely damaged under four-kg TNT explosive, as shown in Figs. 14 and 15 and as presented in Table 1.

Using one-kg TNT explosive charge, the maximum displacement of the lower RC slab at point (4) is computed to discuss the impact of the helical springs, as presented in Table 1. The maximum displacement of the lower RC slab at point (4) is also obtained by the field blast test as presented in Table 1. The result indicates that the helical springs built on the core space of the DRC panel protect the lower reinforced concrete slab from damage, as shown in Figs. 16 and 17 and as

presented in Table 1.

Using five-kg TNT explosive charge, the maximum displacement of the lower RC slab at point (4) is computed to discuss the impact of the helical springs, as presented in Table 1. The maximum displacement of the lower RC slab at point (4) is also obtained by the field blast test as tabulated in Table 1. The result indicates that the helical springs built on the core space of the DRC panel also protect the lower reinforced concrete slab from damage, as shown in Figs. 18 and 19 and as presented in Table 1.

Using ten-kg TNT explosive charge, the maximum displacement of the lower RC slab at point (4) is computed to discuss the impact of the helical springs as tabulated in Table 1. The maximum displacement of the lower RC slab at point (4) is also obtained by the field blast test, as tabulated in Table 1. The result again reveals that the helical springs built on the core space of the DRC panel protect the lower reinforced concrete slab from damage, as shown in Figs. 20 and 21 and as presented in Table 1. However, the helical spring could absorb the blast wave energy to protect the fortified structure. The strain energy of the helical springs between the DRC panels is too high to absorb the blast wave energy. The blast wave energy hitting the protection layer of the DRC panel gives high kinetic energy for it. The helical springs could absorb the kinetic energy of the protection slab to protect the fortified slab from damage.

## **6. Discussions**

The difference between the performance of the lower reinforced concrete slab for the double reinforced concrete panel with and without the helical springs lies in the use of the helical springs. The double reinforced concrete panel (Fig. 3) is used to discuss the impact of the helical springs on the performance of the lower reinforced concrete slab required protecting from blast effect (fortified slab). The field blast test is conducted to study the performance of the DRC panel strengthened by the helical springs and to trace the pressure-time histories hitting the DRC panel based on different TNT explosive charges. The pressure-time history hitting the DRC panel and the maximum displacement of the lower reinforced concrete slab of the DRC panel are recorded. The trends of the pressure-time histories obtained by both the field blast test and the numerical model are the same trend as those presented by Gaissmaire (2003). Based on the field blast test, there is a good agreement between the recorded and the computed maximum displacement of the lower reinforced concrete slab of the DRC panel. The FEA gives a better estimation of the response of the DRC panel strengthened by the helical springs.

Based on the field blast test, the upper reinforced concrete slab (protection slab) and the helical springs can absorb the blast wave to protect the lower of the reinforced concrete slab (fortified slab).

In general, the upper reinforced concrete slab and the helical springs play an important role to resist the blast load. The helical springs improves the performance of the fortified reinforced concrete slab (lower reinforced concrete slab). Therefore, the stiffness of helical springs absorbs the blast wave energy and then the springs reduce the displacement of the fortified reinforced concrete slab compared to the reinforced concrete slabs without the helical springs. The helical springs have a large amount of strain energy which can absorb the kinetic energy of the blast wave propagation. Based on the field blast test and the FEA, the springs existed between the reinforced concrete slabs reduce the maximum displacement of the lower reinforced concrete slab by up to 60%.

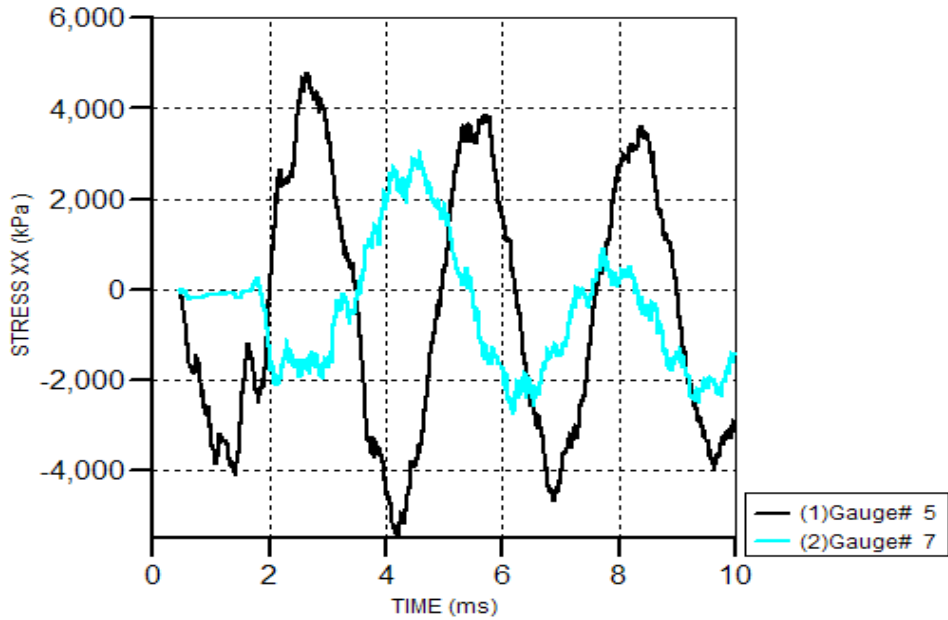


Fig. 23 Stress–time histories of points 5 and 7 located at the DRC panels subjected to 1-kg TNT explosive at stand-off distance (R) of 1 m

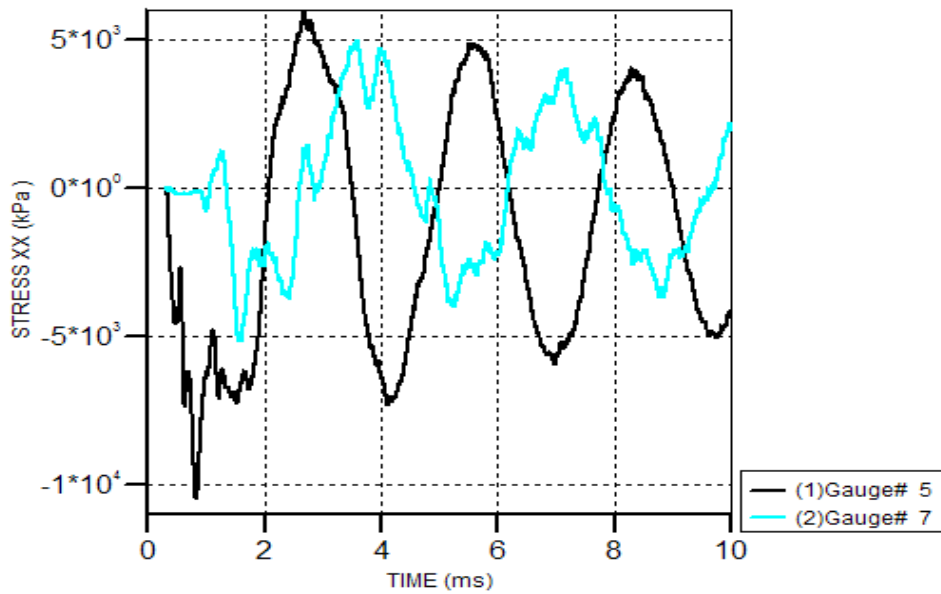


Fig. 24: Stress–time histories of points 5 and 7 located at the DRC panels subjected to 5-kg TNT explosive at stand-off distance (R) of 1 m

Finally, the performance of the lower reinforced concrete slab is highly dependent on the mechanical properties (spring stiffness) of the helical springs which are used as a structural retrofitting system, as shown in Fig. 22. Figs. 23, 24 and 25 show the stresses applied on the upper

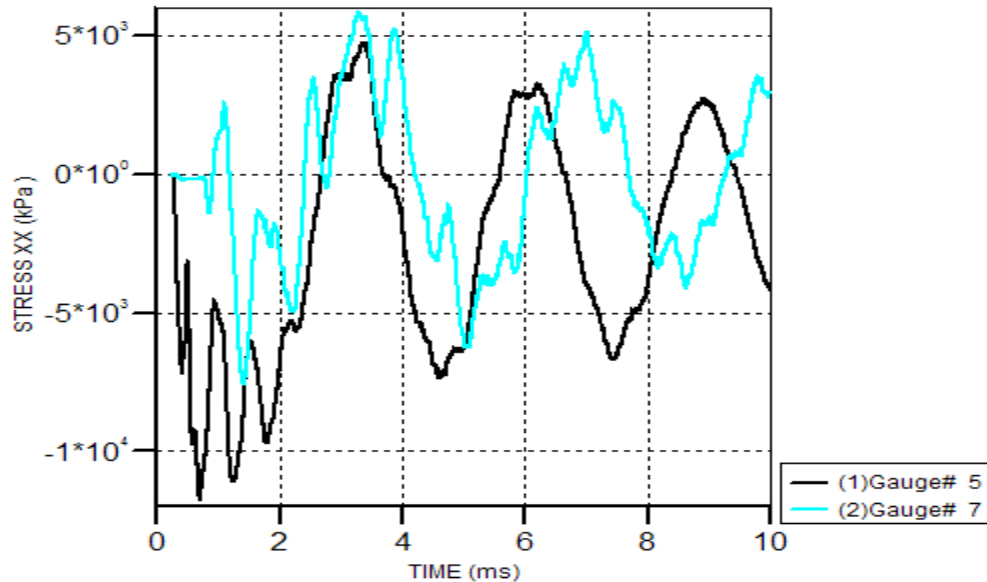


Fig. 25 Stress-time histories of points 5 and 7 located at the DRC panels subjected to 10-kg TNT explosive at stand-off distance (R) of 1 m

reinforced concrete slab of the DRC panel at gauge (5) which is located at the centre of the upper reinforced concrete slab. Figs. 23, 24 and 25 also show the stresses applied on the lower reinforced concrete slab of the DRC at gauge (7) which is located at the centre of the lower reinforced concrete slab. The stresses at the points (5) and (7) located at the DRC panel is computed based on 1-kg , 5-kg , and 10-Kg TNT explosives at a stand-off distance of 1 m, as shown in Fig. 22. The difference between these two stresses has an average value equal to 60%. However, the spring of the DRC panel system could reduce the value of the stress developed at point (7) by up to 60%.

## 7. Conclusions

The field blast test is conducted to study performance of the double reinforced concrete panel strengthened the helical springs existed between the double reinforced concrete panel. A 3-D numerical model is also used to predict the performance of the DRC panel strengthened the helical springs under the blast effect. In this study, the performance of the DRC panel strengthened by the helical springs is modelled and analyzed using the 3-D FEA. The following conclusions can be drawn regarding the performance of the DRC panel strengthened by the helical springs under the impact of the TNT explosives.

- Based on the field blast test and the numerical model, the 3-D numerical model gives a better estimation of the pressure-time history hitting the double reinforced concrete panel.
- The 3-D finite element model can be successfully used to analyze and estimate the performance of the double reinforced concrete panel strengthened by the helical springs based on the field blast test.
- The responses of the DRC panels strengthened by the helical springs are reduced up to 60% with respect to those of the DRC panels without the helical springs.

- The double reinforced concrete panel strengthened by the springs can resist repetitive blast loads to protect the fortified reinforced concrete panels.
  - The upper reinforced concrete slab can be replaced with a new one when it reached to failure state under the blast effect. However, the helical springs and the lower reinforced concrete slab can be again used with the new upper reinforced concrete slab.
- Therefore, the double reinforced concrete panel including the helical springs can be used as structural retrofitting to absorb the energy of the blast wave propagation hitting the fortified reinforced concrete slabs.

## Acknowledgment

The authors acknowledge the Egyptian Engineering Department. Part of the funding for this research is provided by Military Technical College, Technical Research Centre, and the Egyptian Engineering Department.

## References

- Aimone C.T. (1982), "Three-dimensional wave propagation model of full-scale rock fragmentation", Ph.D. Thesis, Northwestern University.
- Asha P. and Sundarajan R. (2014), "Experimental and numerical studies on seismic behavior of exterior beam-column joints", *Comput. Concrete*, **13**(2), 221-234.
- AUTODYN, (2005), *Theory Manuals*, Version 6.1, Century Dynamics Inc., Sam Ramon, USA.
- Baker, W.E., Cox, P.A., Kulesz, J.J. and Strehlow, R.A. (1983), *Explosion hazards and evaluation*, Elsevier.
- Bencardino, F. and Condello, G. (2014), "Experimental and numerical investigation of behavior of RC beams strengthened by steel reinforced grout", *Comput. Concrete*, **14**(6), 711- 725.
- Beshara, F.B.A. (1994), "Modeling of blast loading on aboveground structures -I. Internal blast and ground shock", *Comp. Struct.*, **51**(5), 597-606.
- Chen, H. (Roger) and Chen, S. (1996), "Dynamic responses of shallow-buried flexible plates subjected to impact loading", *J. Struct. Eng.*, January, 55-60.
- Dharmasena, K.P., Wadley, H.N., Xue, Z., John, W. and Hutchinson, J.W. (2008), "Mechanical response of metallic honeycomb sandwich panel structures to high-intensity dynamic loading", *Int. J. Impact Eng.*, **35**(9), 1063-1074.
- Fayad, H.M. (2009), "The optimum design of the tunnels armoured doors under blast effects", Ph. D. Thesis, Military Technical College (MTC), Cairo.
- Gaissmaiere, A.E.W. (2003), "Aspects of thermobaric weapon", *ADF Health*, **4**, 3-6.
- Gustafsson, R. (1973), *Swedish blasting technique*, Gothenburg, Sweden, SPI.
- Ha, J., Yi, N., Choi, J. and Kim, J. (2011), "Experimental study on hybrid CFRP-PU strengthening effect on RC panels under blast loading", *J. Compos. Struct.*, **93**(8), 2070-2082.
- Hao, H., Ma, G.W. and Zhou, Y.X. (1998), "Numerical simulation of underground explosions", *Fragblast Int. J. Blasting Fragmentation*, **2**(4), 383-395.
- Laine, L. and Hedman O. (1999), *Finite element calculation of Swedish rescue centers (RC 90) and shelters*, 3rd Asia-Pacific Conference on Shock & Impact Loads on Structures, 205-212, November 24-26, Singapore.
- Liu, L. and Katsabanis, P.D. (1997), "Development of a continuum damage model for blasting analysis, *Int. J. Rock Mech. Min. Sci.*, **34**(2), 217-231.
- Lu, Y., Wang, Z. and Chong, K. (2005), "A comparative study of buried structure in soil subjected to blast load using 2-D and 3-D numerical simulations", *J. Soil Dyn. Earthq. Eng.*, **25**(4), 275-288.

- Luccioni, B., Ambrosini, D., Nurick, G. and Snyman, I. (2009), "Craters produced by underground explosions", *J. Comput. Struct.*, **87**(21), 1366- 1373.
- Marzec, I., Tejchman, J. and Winnicki, A. (2015), "Computational simulations of concrete behavior under dynamic conditions using elasto-visco-plastic model with non-local softening", *Comput. Concrete*, **15**(4), 515- 545.
- Ming Wei Hsieh (2008), "Investigation on the blast resistance of a stiffened door structure", *J. Marine Sci. Tech.*, **16**(2), 149-157.
- Mohamad, L.S. (2006), "Study and design of fortified structures due to blast effects", M. Sc thesis. Military Technical College (MTC), Cairo. Ammunition and Explosives. In document: AC/258-D/258, Brussels, Belgium.
- Rashad, M. (2014), "Study the behavior of composite sandwich panels under explosion using finite element method", M. Sc. Thesis, Military Technical College (MTC), Cairo.
- Remennikov, A. (2003), "A review of methods for predicting bomb blast effects on buildings", *J. battlefield Tech.*, **6**(3), 155- 161.
- Schueller, C.T. (1991), *Structural dynamics*, Springer-Verlag, Berlin, New York.
- Smith, P.D. and Hetherington, J.G. (1994), *Blast and ballistic loading of structures*, Butterworth-Heinemann Ltd, UK.
- Technical Manual TM 5-1300 (2008), *Structures to Resist the Effects of Accidental Explosions, Unified Facilities Criteria (UFC)*, U.S. Army Corps of Engineers; Naval Facilities Engineering Command; Air Force Civil Engineer Support Agency.
- Technical Manual TM 5-885-1 (1986), *Fundamentals of protective design for conventional weapons*, Headquarters Department of the Army, Washington DC.
- Trelat, S., Sochet, I., Autrusson, B., Cheval, K. and Loiseau, O. (2007), "Impact of a shock wave on a structure on explosion at altitude", *J. Loss Prevention on the process Ind.*, **20**(4), 509-516.
- Wu, C., Hao, H. and Zhou, Y.X. (1999), "Dynamic response analysis of rock mass with stochastic properties subjected to explosive loads", *Fragblast Int. J. Blasting Fragment.*, **3**(2), 137-153.
- Yaghin, M.L., Shahinpar, R. and Ahmadi, H. (2009), "Dynamic behavior of damaged reinforced concrete beams and application of white noise analysis to crack detection", *J. South African Inst. Civil Eng.*, **51**(2), 2-10.
- Zhang, W. and Valliappan, S. (1990), "Analysis of random anisotropic damage mechanics problems of rock mass, Part II: Statistical Estimation", *Rock Mech. Rock Eng.*, **23**(2), 241-259.